Surface Science 646 (2016) 19–25

Contents lists available at ScienceDirect

Surface Science

journal homepage: www.elsevier.com/locate/susc

Oxidation of the Ru(0001) surface covered by weakly bound, ultrathin silicate films

Emre Emmez [a], J. Anibal Boscoboinik [b,*], Samuel Tenney [b], Peter Sutter [b], Shamil Shaikhutdinov [a,*], Hans-Joachim Freund [a]

[a] Abteilung Chemische Physik, Fritz-Haber Institut der MPG, Faradayweg 4-6, 14195 Berlin, Germany
[b] Center for Functional Nanomaterials, Brookhaven National Laboratory, Upton, NY 11973-5000, United States

ARTICLE INFO

Available online 30 June 2015

Keywords:
Ultrathin oxide films
Surface oxidation
Ru oxide
Passivation

ABSTRACT

Bilayer silicate films grown on metal substrates are weakly bound to the metal surfaces, which allows ambient gas molecules to intercalate the oxide/metal interface. In this work, we studied the interaction of oxygen with Ru(0001) supported ultrathin silicate and aluminosilicate films at elevated O_2 pressures (10^{-5}–10 mbar) and temperatures (450–923 K). The results show that the silicate films stay essentially intact under these conditions, and oxygen in the film does not exchange with oxygen in the ambient. O_2 molecules readily penetrate the film and dissociate on the underlying Ru surface underneath. The silicate layer does however strongly passivate the Ru surface towards RuO_2(110) oxide formation that readily occurs on bare Ru(0001) under the same conditions. The results indicate considerable spatial effects for oxidation reactions on metal surfaces in the confined space at the interface. Moreover, the aluminosilicate films completely suppress the Ru oxidation, providing some rationale for using crystalline aluminosilicates in anti-corrosion coatings.

1. Introduction

Silicate and aluminosilicate thin films grown on metal substrates have recently received considerable attention as well-defined models for studying surface chemistry of silica-based materials, in particular of zeolites, as well as crystal–glass transitions exemplified by silica [1–4]. It is well established that the thinnest silica film forms a hexagonal layer of corner-sharing [SiO_4] tetrahedra (referred to as "silicatene" in analogy to graphene [5]) which is strongly bound to a metal support through Si-O-Metal linkages [6]. On noble metals such as Ru(0001), Pd(100) and Pt(111), double-layer (or bilayer) silicate films may be grown, which are weakly bound to the support via dispersive forces [7–10]. In this case, a relatively large space between the silicate sheet and the metal support allows, in principle, small molecules to intercalate the interface, diffuse and ultimately react on the metal surface. Despite being potentially interesting, the studies on chemical reactions in such confined spaces remain in its premature state. To date, only a few studies have been reported for metal-supported graphene [11,12]. In this respect, metal-supported bilayer silicate films, which combine an ultrathin "membrane" and a chemically active metal surface underneath, may become interesting hybrid materials, in particular in catalysis as the silica is a robust material in catalytically relevant atmospheres. (For brevity, we will use "silicate" for the bilayer silicate films studied here).

Obviously, a general scenario for chemical reactions over silicate/metal system exposed to ambient gases must include: (i) penetration of molecules through "pores" in the film; (ii) chemisorption on the metal surface right behind the pore and subsequent diffusion across the metal surface; (iii) surface reactions, and finally (iv) desorption of products (if any) back through the pores in the film. Recently, we have addressed steps (i) and (ii) with respect to CO and D_2 [13]. The results showed that a perfect crystalline silicate (which is represented by a honeycomb-like structure of 6-membered rings) is, in essence, impermeable even for these small molecules. Their penetration seems to occur through the pores associated with large N-membered rings present in the amorphous portion of the films.

In continuation of this work, here we address reactions of silicate/Ru(0001) with molecular oxygen. It has been previously shown that the "as prepared" silicates grown on Ru(0001) commonly contain oxygen atoms adsorbed directly on the metal surface [9,14]. The amount of adsorbed oxygen may be reduced by annealing in ultra-high vacuum (UHV) and recovered by re-oxidation, without changing the structure of the silicate films. As the Ru(0001) surface is prone to form oxidic structures, which are considered as the active phase in catalytic reactions [15], we focus here on oxidation of the Ru(0001) surface underneath the film in more detail, in particular at high O_2 pressures and elevated temperatures.

It is well known that chemisorbed oxygen on Ru(0001) forms several ordered overlayers, e.g. (2 × 2)-O, (2 × 1)-O, (2 × 2)-3O, and (1 × 1)-O.

* Corresponding authors.
E-mail addresses: jboscoboinik@bnl.gov (J. Anibal Boscoboinik), shaikhutdinov@fhi-berlin.mpg.de (S. Shaikhutdinov).

http://dx.doi.org/10.1016/j.susc.2015.06.019
0039-6028/

Further oxidation of the Ru(0001) surface, resulting in the O uptake of more than a monolayer, has been intensively studied since this so-called "oxygen-rich" Ru(0001) surface was found to be very active in CO oxidation [16]. Böttcher and co-workers discussed this surface in terms of subsurface oxygen species [17,18]. However, Over and co-workers clearly demonstrated the formation of a RuO_2(110) thin film on Ru(0001) which may coexist with O(1 × 1)-Ru(0001), depending on the preparation conditions [19–21]. Further studies showed that it is adsorbed oxygen atoms located in terminal position above the coordinatively unsaturated Ru sites on RuO_2(110) that is involved in CO oxidation [22–25]. Nonetheless, it is fair to say that chemisorbed oxygen, surface oxides, buried oxides, and subsurface oxygen may, in principle, all coexist in the near surface region of Ru(0001), thus leading to a rich oxygen-ruthenium surface chemistry [15,26]. Indeed, a low energy electron microscopy study on the oxidation of Ru(0001) revealed the substantial spatial inhomogeneity in the oxide formation across the surface [27].

2. Materials and methods

Experiments were carried out in two different UHV setups located in Fritz Haber Institute and Brookhaven National Laboratory. The first chamber (base pressure 2×10^{-10} mbar) is equipped with low-energy electron diffraction (LEED), Auger electron spectroscopy (AES), infrared reflection–absorption spectroscopy (IRAS), and a quadrupole mass-spectrometer for temperature programmed desorption (TPD) experiments.

The Ru(0001) crystal (10 mm in diameter, 1.5 mm thick, from MaTeck) is spot-welded to the two parallel Ta wires used for resistive heating as well as sample cooling by filling the manipulator rod with liquid nitrogen. The temperature was measured by a type K thermocouple spot-welded to the backside of the crystal. Silicate films were grown on the Ru(0001) surface as described in detail elsewhere [9]. Briefly, silicon was vapor deposited from a Si rod (99.999%, Goodfellow) onto oxygen precovered 3O(2 × 2)-Ru(0001) surface at ~100 K, followed by oxidation at ~1250 K in 10^{-6} mbar O_2 for 10 min. For the preparation of aluminosilicate films, Si and Al (99.999%, Goodfellow) were co-deposited onto oxygen precovered Ru(0001) at ~100 K (in total amounts equal to the amount of Si necessary to prepare a pure silicate film) and then oxidized at ~1200 K for 10 min [2].

Exposure to gases at pressures in the mbar range was performed in a separate high-pressure cell sealed from the UHV chamber by a Viton O-ring. After the treatment, the cell was pumped down to 10^{-7} mbar before the sample was transferred back to the UHV chamber. For O_2 (99.9995%) exposures, a cold trap was used to prevent contamination at elevated pressures.

The mass spectrometer had a differentially pumped shield with an aperture of 6 mm. For the TPD measurements, the nozzle of the shield was placed about 0.5 mm in front of the sample surface to minimize the signal coming from the sample heating wires. TPD spectra were measured at a heating rate of 3 K/s. The IRA-spectra were recorded using p-polarized light at 84° grazing angle of incidence (resolution 4 cm^{-1}).

The second UHV system is an Ambient Pressure X-ray Photoelectron Spectroscopy (AP-XPS) setup at beamline X1A1 of the National Synchrotron Light Source (NSLS) that uses a differentially pumped hemispherical analyzer (Specs Phoibos 150 NAP) equipped with a CEM 9 channeltron detector and a 300 μm entrance aperture to the first differential pumping stage. The sample was positioned ~0.6 mm from the aperture to ensure that the local pressure at the surface was not significantly affected by the differential pumping through the aperture. The analyzer was offset by 70° from the incident X-ray beam and 20° from the surface normal of the sample. A photon energy of ~580 eV was used in the experiments reported here, which gives similar mean free paths for Ru 3d (~6 Å) and O 1s (~5 Å) core levels, according to calculations reported for Ru in ref. [28]. The aluminosilicate film was prepared on Ru(0001) with a composition $Al_{0.2}Si_{0.8}O_2$, following the recipe described in ref. [2]. The crystal was mounted on a ceramic button heater to allow heating at elevated oxygen pressures. The temperature was measured with a type K thermocouple in contact with the sample.

3. Results and discussion

3.1. Pure silicate films

As previously shown, [14] the "as grown" films contain O atoms directly chemisorbed on Ru(0001). Combined TPD and IRAS studies showed that these O ad-atoms suppress CO and D_2 adsorption even after UHV annealing at 1275 K [13]. In order to get rid of O species from the Ru(0001) surface underneath the film via chemical reaction, the sample was exposed to high pressures of H_2 (1 mbar, 470 K). Subsequent CO and D_2 adsorption experiments showed spectral features characteristic of the clean Ru(0001) surface underneath the silica film. However, O_2 exposure (~150 L) to the resulted films at 300 K again suppresses CO and H_2 uptakes, thus suggesting that molecular oxygen readily reaches the Ru(0001) surface and dissociates at 300 K.

Oxidation of Ru(0001) resulting in the O uptake of more than a monolayer requires elevated pressures and temperatures. Commonly, thin RuO_2(110) films are prepared by exposing Ru(0001) to high doses of molecular oxygen at 10^{-6}–10^{-4} mbar and elevated temperatures [22,23,29,30]. In this study, we oxidized Ru(0001) in 10^{-5} mbar of O_2 at 700 K for 45 min, and sample cooling to room temperature was performed in the same oxygen ambient. This procedure results in a characteristic LEED pattern of RuO_2(110)/Ru(0001) that has been well-documented in the literature [20]. Nominal film thicknesses could be estimated from Auger O (at 510 eV) and Ru (at 280 eV) signal ratios (~0.7, see top spectrum in Fig. 1b), which corresponds to about 6 ML of O, based on our calibration using 3O(2 × 2)-Ru(0001) surface as a benchmark [29]. In addition, thermal desorption of O_2 from the resulted surface, shown in Fig. 1a, nicely reproduces previously reported TPD spectra of RuO_2(110) [22], showing two peaks at ~400 and ~1005 K. The high temperature peak is associated with Ru-oxide film decomposition, whereas the weakly bonded oxygen species (at ~400 K) are assigned to adsorbed oxygen atoms located in terminal positions above the coordinatively unsaturated Ru sites on RuO_2(110) [22].

Now we address the results of oxidation of silicate-covered Ru(0001). Note that the "as grown" silicate film does not show any considerable oxygen desorption below 1200 K (Fig. 1a, green curve). As silicate itself does not decompose or dewet at these temperatures as judged by IRAS [13], the small desorption signal above ~1100 K could be assigned to the onset of oxygen desorption from the Ru(0001) surface underneath, which fully occurs only at temperatures as high as 1400 K [17].

The silicate-covered Ru(0001) sample was then exposed to the same conditions as used above for the preparation of RuO_2(110) films (i.e. 10^{-5} mbar O_2 at 700 K for 45 min). The corresponding TPD spectrum (Fig. 1a, red curve) revealed two desorption signals which resemble those observed upon oxidation of pure Ru(0001). In principle, this finding suggests the formation of a Ru-oxide film underneath the silicate, although it is strongly suppressed, as the integral intensity of the high temperature peak associated with the decomposition of Ru-oxide is a factor of ~3 lower than that of observed on the Ru(0001) sample. Accordingly, AES inspection (Fig. 1b) showed only slight increase in the O(510 eV)/Ru(280 eV) signal ratio (0.25 vs 0.21 for the oxidized and the "as grown" silicate samples, respectively), which is much lower than 0.7 observed for pristine Ru(0001) under these conditions.

Further comparison of TPD spectra obtained for these two surfaces revealed considerable qualitative differences. Notably, the onset of high-temperature desorption on oxidized silicate/Ru is shifted towards higher temperatures by about 40 K. As the desorption profile may be also coverage dependent, one should, in principle, compare the spectra at the same oxygen coverage. However, following the TPD results of

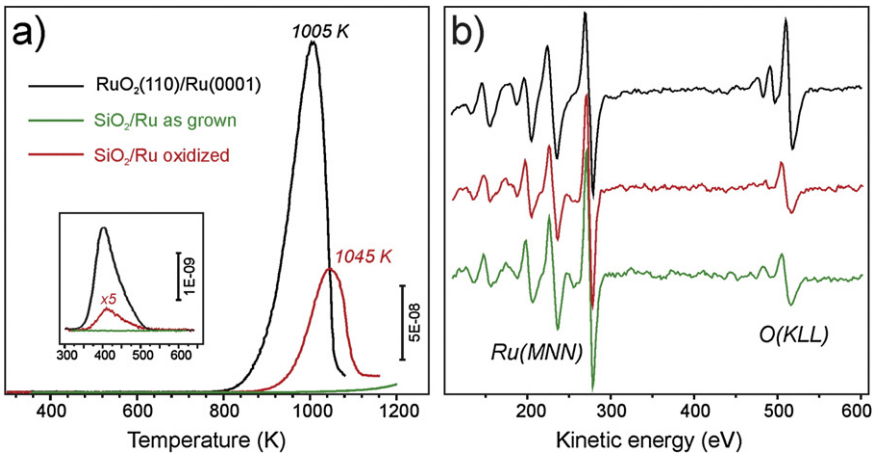

Fig. 1. O_2-TPD spectra (a) and AES spectra (b) of Ru(0001) (in black) and SiO_2/Ru(0001) (in red) surfaces after exposure to 10^{-5} mbar O_2 at 700 K for 45 min. The results for "as grown" SiO_2/Ru(0001) (in green) are shown for comparison.

Böttcher and coworkers of bare Ru(0001) [17], this desorption temperature does not shift much with increasing oxygen content. On the basis of our previous studies of CO and D_2 adsorption showing such shifts at nearly the same coverages [13], the shift observed in Fig. 1a can be explained in a similar way by that oxygen molecules, produced upon decomposition of Ru-oxide, need some time to find the pores in silicate to escape. As a result, the desorption is delayed as compared to uncovered Ru(0001), and as such appeared at higher temperatures in TPD spectra. Interestingly, such a delay observed here for O_2 (~40 K) is almost the same as previously observed for D_2, and both are considerably larger than obtained for CO (~25 K), most likely because of $O_2(D_2)$ desorption additionally includes O(D) recombination and hence time.

On the other hand, the low-temperature desorption peak at ~400 K does not exhibit such a shift. Moreover, its intensity is a factor of ~25 lower, whereas a factor ~3 is obtained for the high temperature peak. Since the weakly bonded state is associated with the $RuO_2(110)$ surface, we conclude that the Ru-oxide formed underneath silicate exposes other terminations. As LEED inspection did not reveal any ordered structures, the resulting Ru-oxide film is amorphous in nature.

On the basis of these results, we may speculate on the following scenario. Apparently, the "as grown" silicate films possess some amounts of "holes" or large "pores". The Ru surface behind these pores behaves, in essence, like uncovered Ru(0001). Upon oxidation, these areas transform into $RuO_2(110)$ that gives rise to the low temperature desorption peak at nearly the same temperature as that observed for extended $RuO_2(110)$/Ru(0001). Based on the signal intensity ratio in pure and silicate covered Ru samples, one can estimate such domains to cover about 4% of the entire surface, whereas the majority of Ru-oxide, which is of about 2 ML in nominal thickness as estimated from the high temperature signal ratios, is present in the amorphous state. It remains unclear, however, whether this oxide film uniformly covers the Ru support or is preferentially formed in the proximity to the pores in a silicate film responsible for the oxygen permeation.

In the next set of experiments, we studied oxidation at high oxygen pressures. Again, we first address the results for the clean Ru(0001) surface, which was exposed to 15 mbar O_2 at 700 K for 45 min and cooled down in oxygen to 300 K before oxygen was pumped away. Fig. 2a shows O_2 desorption spectrum (in black) from the resulting surface. Not surprisingly, the total amount of O_2 molecules desorbing at high temperatures increased substantially (by factor of 4.5) as compared to that observed after oxidation in 10^{-5} mbar of O_2, therefore indicating progressive oxidation of the deeper layers of Ru(0001) at elevated pressures. On the other hand, the intensity of a weakly bonded state at ~400 K, which is characteristic for the $RuO_2(110)$ terminated surface,

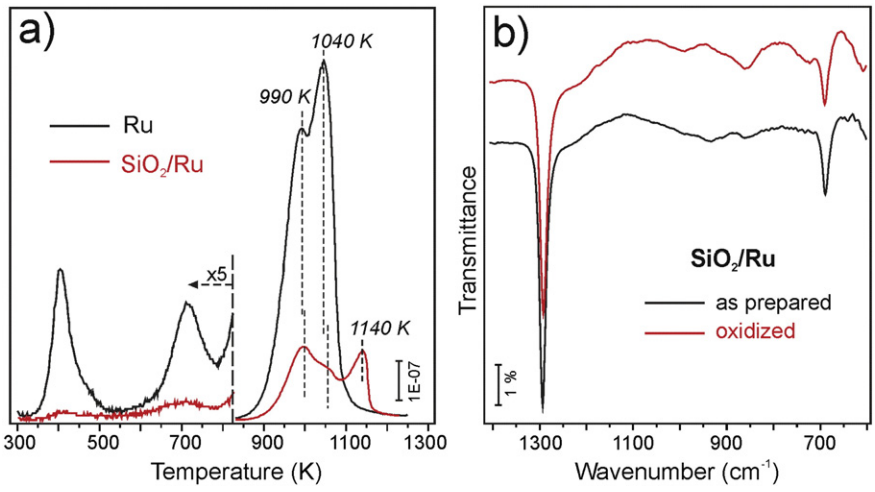

Fig. 2. (a) O_2 (32 amu) signals in TPD spectra of Ru(0001) (in black) and SiO_2/Ru(0001) (in red) surfaces after exposure to 15 mbar O_2 at 700 K for 45 min. (b) IRA-spectra of the SiO_2/Ru(0001) film before (in black) and after (in red) oxygen exposure show that the structure of the silicate film is maintained.

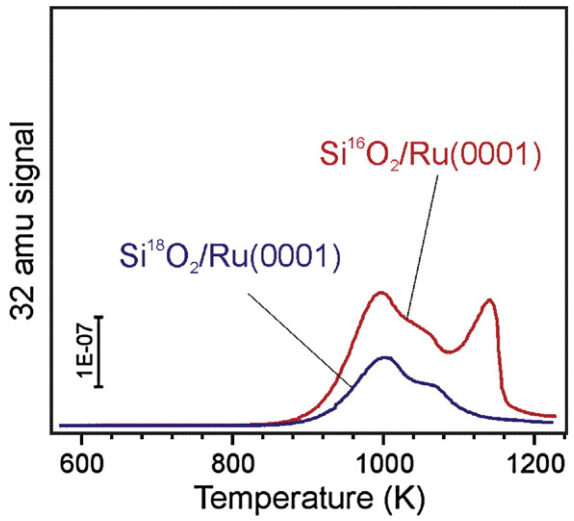

Fig. 3. Oxygen (32 amu) signal in TPD spectra of SiO_2/Ru(0001) films prepared with ^{16}O and ^{18}O isotopes as indicated. Both films were then exposed to 15 mbar $^{16}O_2$ at 700 K for 45 min. Note that the ^{18}O-labeled film additionally contained silica nanoparticles (see Fig. S2 in Supporting Information).

is *reduced* by factor of ~3.5. In addition, a new desorption feature is seen at 710 K, and the most intense high temperature signal clearly shows two peaks at 990 and 1040 K, respectively.

To the best of our knowledge, TPD spectra of Ru(0001) exposed to near-atmospheric oxygen pressures have only been reported by Böttcher and co-workers [18]. Similar to our spectra, two well-separated TPD features at about 1000 and 1050 K (O_β, and O_α, in their notation) were observed upon exposure of Ru(0001) to 1 bar O_2 at 350–450 K, although the precise peak positions deviate depending on the O_2 dosage (in the range of 10^{11}–10^{14} L) and adsorption temperature. The authors assigned these features to substantial amounts of oxygen (~3.5 ML) incorporating into the subsurface region without creating the RuO_2 phase. This conclusion has been drawn on the basis of LEED patterns showing only Ru(0001)-(1 × 1) diffraction spots, and the lack of a desorption state at 400 K which they considered as a fingerprint for RuO_2. Upon exposure to 1 bar O_2 at higher temperatures (500–550 K), a new state (O_γ, in their notation) at 1120 K developed, which was assigned to the initial formation of RuO_2 nuclei that progressively grew in size, and the O_γ peak dominated the TPD spectra. Concomitantly, characteristic RuO_2(110) spots appeared in LEED patterns.

Unfortunately, this paper [18] does not provide O_2-TPD spectra below 800 K to compare with a weak signal at 710 K observed here (Fig. 2a). Nonetheless, on the basis of its low intensity, this feature seems to be associated with surface rather than bulk O species. To some extent, similar desorption features have recently been reported by Over and co-workers [31] in the course of the initial oxidation of Ru(0001) at room temperature using atomic oxygen as the oxidizing agent, which assigned this feature at ~700 K to Ru oxide clusters formed preferentially at step edges. (Note that the sample temperature could not be accurately measured in this study, see ref. [32]). Certainly, such assignment can hardly be applied here for heavily oxidized Ru surface.

It is also noteworthy to discuss here the origin of the oxygen desorption at ~400 K. It appears that this feature is characteristic exclusively for the RuO_2(110) surface. Indeed, such a signal was not observed on disordered RuO_2 films, grown on Pt(111) to the same (~6 ML) film thickness as on Ru(0001) as judged by AES (see Fig. S1 in the Supporting Information). The films were prepared by Ru deposition in 5×10^{-7} mbar O_2 at 300 K and subsequent oxidation in 2×10^{-4} mbar at 700 K for 40 min, i.e. under conditions which normally resulted in RuO_2(110) films on Ru(0001). However, none of the films prepared on Pt(111) shows weakly bonded O species at 400 K, even after exposure to 20 mbar O_2. Instead, additional TPD signals were observed at ~800 K and ~1160 K, which were missing on RuO_2(110)/Ru(0001) after the same treatment (Fig. S1). Therefore, the lack of oxygen desorption at ~400 K does not mean the absence of a Ru-oxide phase, but solely the absence of the RuO_2(110) surface. Accordingly, exposure of Ru(0001) to 15 mbar O_2 at 700 K in our experiments most likely results in a mixture of several Ru-oxide phases, which may expose the RuO_2(110) surface as well as other yet undefined surfaces possessing oxygen atoms which desorb at 710 K and 1140 K (Fig. 2a). Interestingly, for the RuO_2(110) films on Ru(0001)[29] and the RuO_x films on Pt(111) (Fig. S1), all treated with 20 mbar O_2 at 450 K, the O_2 desorption at ~1000 K showed a single peak, whereas a double peak is observed here (Fig. 2a) for oxidation at higher temperatures (700 K vs 450 K). It seems plausible, that all oxygen desorption features at T > 900 K are associated with decomposition of different Ru-oxide phases, in which formation and/or phase separation depends on oxygen pressure and temperature.

Now we address the results of the high-pressure oxidation of silicate-covered Ru(0001). The TPD spectrum revealed the same

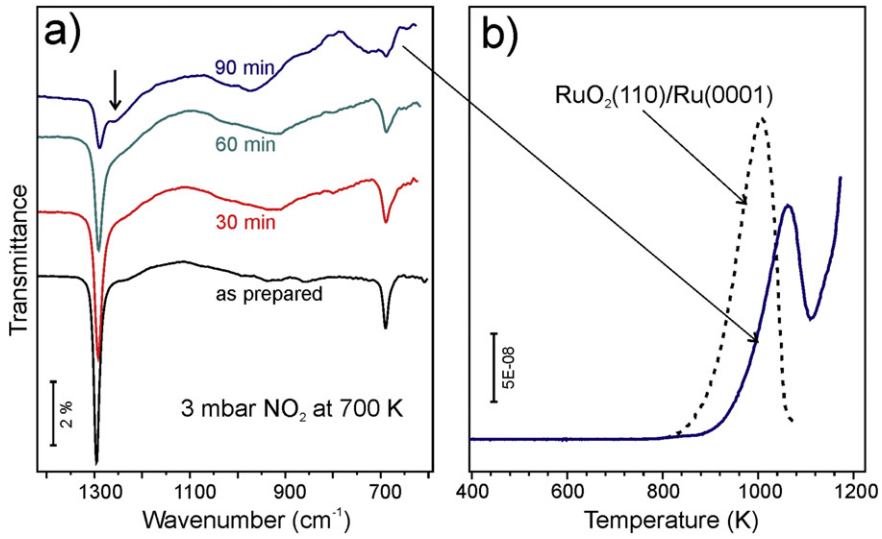

Fig. 4. (a) IRA-spectra of SiO_2/Ru(0001) after stepwise exposure to 3 mbar NO_2 at 700 K. Total exposure time is indicated. The arrow on panel (a) highlights the feature commonly assigned to three-dimensional silica particles caused by film dewetting. Oxygen TPD spectrum taken for the last sample is shown in (b). TPD spectrum for RuO_2(110)/Ru(0001) from Fig. 1a is shown as dashed line, for comparison.

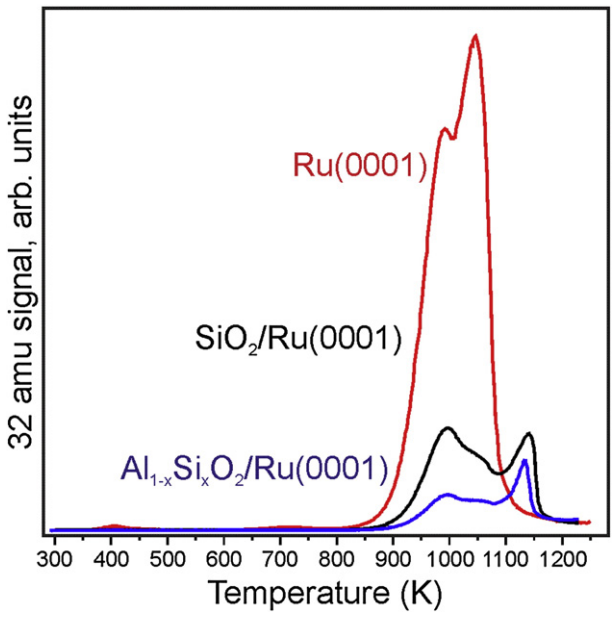

Fig. 5. Comparative TPD spectra of O_2 (32 amu) from three different samples as indicated. All were exposed to 15 mbar of O_2 at 700 K for 40 min.

features as observed on pristine Ru(0001), although of much lower intensity (Fig. 2a), thus suggesting that silicate strongly passivates the Ru(0001) surface even at high oxygen pressures. Comparison of the IRA-spectra before and after oxidation (Fig. 2b) shows that high-pressure treatment does not affect the bilayer structure of the silicate film. Apparently, the silicate film remains decoupled from the support which is oxidized, although to a much lower extent than bare Ru(0001).

However, an additional desorption feature appears at 1140 K, which is missing on pure as well as silicate-covered Ru(0001) at low oxygen pressures (Fig. 1). The desorption feature at 1140 K is only observed upon oxidation at high pressures, and only on silicate-covered Ru(0001). To shed more light on its origin, in particular to see whether this signal could be assigned to decomposition of adventitious silica nanoparticles and clusters, we prepared a sample possessing about 20% more Si than in the "perfect" silicate films. In addition, this film was prepared using isotopically labeled molecular oxygen, $^{18}O_2$. As expected, a new broad band centered at 1190 cm^{-1} is observed in IRA-spectrum which is characteristic for three-dimensional, bulk-like (^{18}O-labeled) silica [1,7,9] (see Fig. S2), suggesting that this sample contains also some silica nanoparticles. The sample was then treated with $^{16}O_2$, and the TPD spectrum was recorded. The results revealed desorption exclusively of $^{16}O_2$ (Fig. 3) and no any traces of $^{18}O_2$ and $^{16}O^{18}O$, thus providing the compelling evidence that oxygen in the silicate film does not scramble with ambient oxygen, and Ru oxide is formed by interaction with ambient oxygen molecules, in full agreement with IRAS results (Fig. 2b) showing that the silicate film remains intact under these conditions.

Surprisingly, the peak at 1140 K has not been observed in this experiment. Taking into account that similar desorption was found on disordered RuO_x films grown on Pt(111) (see Fig. S1), we have tentatively assigned this feature to the desorption from poorly defined Ru-oxide phase(s), which are formed on Ru(0001) only when covered by a "perfect" silicate bilayer film.

Finally, we examined oxidation of silicate-covered Ru(0001) using NO_2 as a stronger oxidizing agent [33]. Fig. 4a shows a series of IRA-spectra upon stepwise exposure to 3 mbar NO_2 at 700 K at the intervals indicated. (The NO_2 was always evacuated for the IRAS measurements). Clearly, principal phonon bands at 1300 and 690 cm^{-1} are gradually attenuated with increasing NO_2 exposure. After a total exposure of 90 min, a prominent shoulder appears as indicated by the arrow in Fig. 4a, which is a clear indication of the film dewetting and formation of three-dimensional silica nanoparticles. AES measurements of the resulted surface revealed an O/Ru signal ratio of 0.5, which is remarkably higher than 0.25 observed for the O_2-treated SiO_2/Ru sample, but still

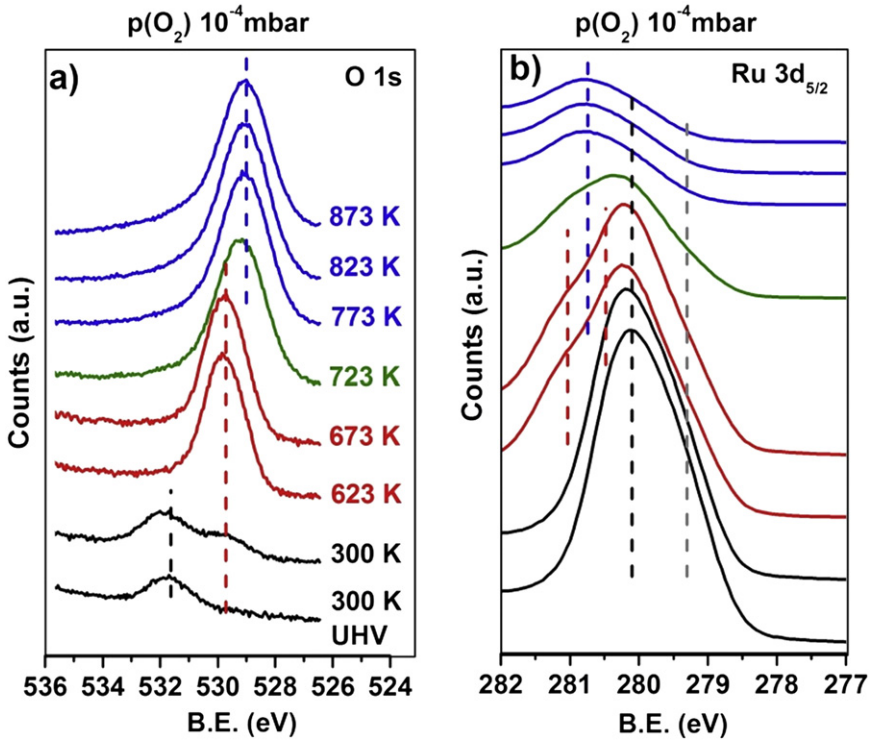

Fig. 6. O 1s (a) and Ru $3d_{5/2}$ (b) regions in AP-XPS spectra taken in 10^{-4} mbar of O_2 at increasing temperatures as indicated. The lowermost spectra are obtained in UHV for the clean Ru(0001) surface prior to the oxygen exposure. The photon energy is 580 eV. The spectra are offset for clarity.

below the 0.7 observed for RuO_2(110)/Ru (see Fig. 1b). TPD spectrum shown in Fig. 4b also confirms deeper oxidation of the Ru support by NO_2 as compared to O_2.

3.2. Aluminosilicate films

Now we turn to the oxidation of aluminosilicate films on Ru(0001). These films are formed by substitution of some Si ions with Al in the bilayer structure and may contain highly acidic, bridging hydroxyl species depending on the Al:Si molar ratio [2]. To compare with pure silicate films, the aluminosilicate film with $Al_{0.25}Si_{0.75}O_2$ composition (as determined by AES) was exposed to 15 mbar of O_2 at 700 K. The typical TPD spectrum is shown on Fig. 5 in direct comparison with pure Ru and silicate/Ru samples. Clearly, there are some similarities in the TPD profiles of pure silicate and aluminosilicate films. However, it is clear that aluminosilicate films suppress oxidation of the Ru surface to the larger extent.

In order to further address the passivation effects of aluminosilicate films, we carried out in situ AP-XPS measurements at BNL (see Experimental). The experiments were performed as to directly compare interaction of oxygen with a bare Ru(0001) surface and with an aluminosilicate film of compositional stoichiometry $Al_{0.2}Si_{0.8}O_2$ as determined by XPS. Unless stated, the spectra were taken in ~10^{-4} mbar O_2 ambient at varying temperature.

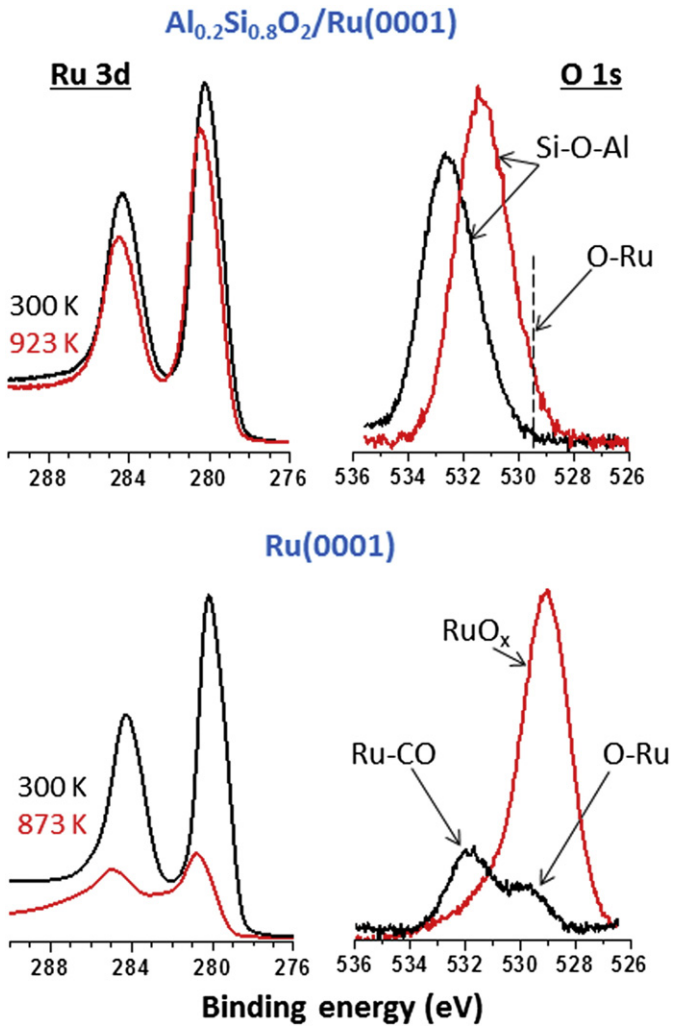

Fig. 7. Ru 3d and O 1s regions in XP-spectra of the bare Ru(0001) surface and the aluminosilicate film measured at 300 K and after heating in 10^{-4} mbar O_2 to the indicated temperatures.

As a starting point, bottom lines in Fig. 6 show the Ru $3d_{5/2}$ and O 1s core level spectra for the clean Ru(0001) surface at 300 K. The Ru $3d_{5/2}$ signal, centered at 280.1 eV, has a shoulder at lower binding energy (BE) (at 279.3 eV) which is attributed to the surface core level shift (SCLS). A small signal at 531.8 eV in the O 1s region originates from CO adsorbed on the surface from the UHV background. Upon O_2 exposure to 10^{-4} mbar at 300 K, the ~529.8 eV signal that appears is assigned to chemisorbed O species. Upon heating to 623 K, this signal gains intensity due to increasing O coverage, ultimately forming an O-(1×1) overlayer [34]. Concomitantly, the SCLS shoulder attenuates and a new feature develops on the higher BE side of the Ru $3d_{5/2}$ peak, which has previously been assigned to Ru coordinated to surface and possibly subsurface oxygen species [35]. No further changes are observed at 673 K. Note, however, that the O 1s signal starts to shift to a lower BE (ultimately, to 529.0 eV) and gains intensity upon further heating to 723 K, thus indicating oxidation of the deeper metal layers. Concomitantly, the Ru $3d_{5/2}$ peak centered at 280.6 eV dominates the spectrum, although the intensity diminishes, in agreement with the formation of a RuO_2 phase.

Spectral deconvolution of the Ru 3d signal measured at 873 K in 10^{-4} mbar O_2 revealed at least three different states coexisting (Figure S3). This finding is in agreement with the presence of different Ru oxide phases deduced on the basis of TPD results in Section 3.1. Note, that for the 580 eV photon energy used here, the inelastic mean free paths of photoelectrons (~6 Å and 5 Å for the Ru 3d and O 1s levels, respectively [28]) limit the probing depth to the first few atomic layers.

Fig. 7 compares the Ru 3d and O1s spectra obtained for the bare and the aluminosilicate-covered Ru(0001) surfaces at 300 K and after heating in O_2 to elevated temperatures. Clearly, the oxidation of Ru(0001) covered by an aluminosilicate film is completely inhibited. In essence, Ru is only observed in a metallic state, although with a slightly (by 0.2 eV) shifted BE. The corresponding O 1s spectra show an ~30% increase in intensity upon heating in O_2 at 923 K. This is assigned to increasing amounts of the interfacial O atoms chemisorbed on Ru(0001) with BE at ~530 eV. Using the amounts of oxygen in the original silicate film as an internal reference for calibration, we estimated the additional interfacial O, formed upon the high-pressure O_2 treatment, to be about 0.6 ML. (Note that this value must be taken as an upper limit since the signal attenuation by atoms in the aluminosilicate film was not taken into account). Also, a prominent shift to lower BEs by ~1.0 eV (from 532.3 to 531.3 eV) is observed (Figure S4), which is related to the changes in the work function (see details in refs. [14,36]). Looking back at the Ru 3d level, the slight decrease in the peak area is related to the addition of the aforementioned chemisorbed oxygen on Ru(0001). This explains as well the 0.2 eV shift by the attenuation of the SCLS. Finally, comparing the Ru $3d_{3/2}$ and the $3d_{5/2}$ peaks, one may find some loss of intensity for the former signal, which is most likely due to burning adventitious carbon in oxygen ambient, as the Ru $3d_{3/2}$ level partially overlaps with the C 1s level.

All in all, the AP XPS results show that oxygen can penetrate the aluminosilicate film and dissociatively chemisorb on Ru(0001). However, further accumulation of oxygen and subsequent oxidation to form Ru-oxide phases is completely inhibited, at least in 10^{-4} mbar of O_2 at 923 K used here.

4. Summary and concluding remarks

Bilayer silicate films grown on metal substrates, which are weakly bound to the metal surfaces, allow ambient gas molecules to intercalate the oxide/metal interface. In this study, we investigated the interaction of oxygen with Ru(0001) supported ultrathin silicate and aluminosilicate films at elevated O_2 pressures (10^{-5}–10 mbar) and temperatures (450–923 K). The results show that the silicate films stay essentially intact under these conditions, and oxygen in the film does not scramble with oxygen in the ambient. Molecular oxygen readily penetrates the film and dissociates on the Ru surface underneath. However, the silicate

layer strongly passivates the Ru surface towards RuO_2(110) oxide formation that readily occurs on bare Ru(0001) under the same conditions. These results indicate considerable spatial effects for oxidation reactions on metal surfaces in the confined space at the interface. Such phenomena have recently received much attention for the case of metal supported graphene and may potentially be interesting in the case of silicates as more robust materials under strongly oxidizing conditions.

Ultrathin aluminosilicate films were found to completely suppress the Ru oxidation. The observed passivation of the metal surface underneath the film may provide some rationale for using aluminosilicates in general, and zeolites in particular, as anti-corrosion coatings for various applications [37,38]. It is noteworthy that the bilayer structure of silicate films studied here is a structural unit of hexacelsian, a layered material from the feldspar family, which is used as an anticorrosion coating [39,40]. It may well be that in the cases of using zeolitic coatings, the zeolite framework collapses into a less permeable, hexacelsian-like layered material, as previously shown for zeolite A treated at high temperatures [41], and for which we have observed structural relationships between the films and zeolites [42].

Acknowledgments

We acknowledge financial support from Deutsche Forschungsgemeinschaft through collaborative research program SFB 1109. E.E. thanks the International Max Planck Research School "Functional interfaces in physics and chemistry" for the fellowship. J.A.B. acknowledges Alexander von Humboldt Foundation for the fellowship while his staying at FHI. We are grateful to Dr. Yu. Martynova for providing us unpublished results for RuO_x films on Pt(111). Research was carried out in part at the Center for Functional Nanomaterials and National Synchrotron Light Source, Brookhaven National Laboratory, which is supported by the U.S. Department of Energy, Office of Basic Energy Sciences, under Contract No. DE-AC02-98CH10886.

Appendix A. Supplementary data

Supplementary data to this article can be found online at http://dx.doi.org/10.1016/j.susc.2015.06.019.

References

[1] S. Shaikhutdinov, H.-J. Freund, Adv. Mater. 25 (2013) 49.
[2] J.A. Boscoboinik, X. Yu, B. Yang, F.D. Fischer, R. Włodarczyk, M. Sierka, S. Shaikhutdinov, J. Sauer, H.-J. Freund, Angew. Chem. Int. Ed. 51 (2012) 6005.
[3] M. Heyde, S. Shaikhutdinov, H.J. Freund, Chem. Phys. Lett. 550 (2012) 1.
[4] J.A. Boscoboinik, S. Shaikhutdinov, Exploring zeolite chemistry with the tools of surface science: challenges, opportunities, and limitations, catalysis letters, 1442014. 1987.
[5] B. Yang, J.A. Boscoboinik, X. Yu, S. Shaikhutdinov, H.-J. Freund, Nano Lett. 13 (2013) 4422.
[6] J. Weissenrieder, S. Kaya, J.-L. Lu, H.-J. Gao, S. Shaikhutdinov, H.-J. Freund, M. Sierka, T.K. Todorova, J. Sauer, Phys. Rev. Lett. 95 (2005) 076103.
[7] D. Löffler, J.J. Uhlrich, M. Baron, B. Yang, X. Yu, L. Lichtenstein, L. Heinke, C. Büchner, M. Heyde, S. Shaikhutdinov, H.J. Freund, R. Włodarczyk, M. Sierka, J. Sauer, Phys. Rev. Lett. 105 (2010) 146104.
[8] X. Yu, B. Yang, J.A. Boscoboinik, S. Shaikhutdinov, H.-J. Freund, Appl. Phys. Lett. 100 (2012) 151608.
[9] B. Yang, W.E. Kaden, X. Yu, J.A. Boscoboinik, Y. Martynova, L. Lichtenstein, M. Heyde, M. Sterrer, R. Wlodarczyk, M. Sierka, J. Sauer, S. Shaikhutdinov, H.-J. Freund, Phys. Chem. Chem. Phys. 14 (2012) 11344.
[10] E.I. Altman, J. Götzen, N. Samudrala, U.D. Schwarz, J. Phys. Chem. C 117 (2013) 26144.
[11] R. Mu, Q. Fu, L. Jin, L. Yu, G. Fang, D. Tan, X. Bao, Angew. Chem. Int. Ed. 51 (2012) 4856.
[12] P. Sutter, J.T. Sadowski, E.A. Sutter, J. Am. Chem. Soc. 132 (2010) 8175.
[13] E. Emmez, B. Yang, S. Shaikhutdinov, H.-J. Freund, J. Phys. Chem. C 118 (2014) 29034.
[14] R. Włodarczyk, M. Sierka, J. Sauer, D. Löffler, J.J. Uhlrich, X. Yu, B. Yang, I.M.N. Groot, S. Shaikhutdinov, H.J. Freund, Phys. Rev. B 85 (2012) 085403.
[15] H. Over, Chem. Rev. 112 (2012) 3356.
[16] A. Böttcher, H. Niehus, S. Schwegmann, H. Over, G. Ertl, J. Phys. Chem. B 101 (1997) 11185.
[17] A. Böttcher, H. Niehus, J. Chem. Phys. 110 (1999) 3186.
[18] R. Blume, H. Niehus, H. Conrad, A. Böttcher, J. Chem. Phys. 120 (2004) 3871.
[19] Y.D. Kim, H. Over, G. Krabbes, G. Ertl, Top. Catal. 14 (2001) 95.
[20] Y.D. Kim, A.P. Seitsonen, H. Over, Surf. Sci. 465 (2000) 1.
[21] H. Over, M. Muhler, Prog. Surf. Sci. 72 (2003) 3.
[22] Y.D. Kim, A.P. Seitsonen, S. Wendt, J. Wang, C. Fan, K. Jacobi, H. Over, G. Ertl, J. Phys. Chem. B 105 (2001) 3752.
[23] S. Wendt, M. Knapp, H. Over, J. Am. Chem. Soc. 126 (2004) 1537.
[24] K. Reuter, M. Scheffler, Phys. Rev. B 68 (2003) 045407.
[25] J. Wang, C.Y. Fan, K. Jacobi, G. Ertl, J. Phys. Chem. B 106 (2002) 3422.
[26] A. Böttcher, U. Starke, H. Conrad, R. Blume, H. Niehus, L. Gregoratti, B. Kaulich, A. Barinov, M. Kiskinova, J. Chem. Phys. 117 (2002) 8104.
[27] J.I. Flege, J. Hrbek, P. Sutter, Phys. Rev. B 78 (2008) 165407.
[28] C.J. Powell, A. Jablonski, NIST Electron Inelastic-Mean-Free-Path Database, Version 1.2, SRD 71, National Institute of Standards and Technology, Gaithersburg, MD, 2010.
[29] Y. Martynova, B. Yang, X. Yu, J.A. Boscoboinik, S. Shaikhutdinov, H.J. Freund, Catal. Lett. 142 (2012) 657.
[30] M. Rössler, S. Günther, J. Wintterlin, J. Phys. Chem. C 111 (2007) 2242.
[31] B. Herd, J.C. Goritzka, H. Over, J. Phys. Chem. C 117 (2013) 15148.
[32] B. Herd, M. Knapp, H. Over, J. Phys. Chem. C 116 (2012) 24649.
[33] W.J. Mitchell, W.H. Weinberg, J. Chem. Phys. 104 (1996) 9127.
[34] H. Over, A.P. Seitsonen, E. Lundgren, M. Wiklund, J.N. Andersen, Chem. Phys. Lett. 342 (2001) 467.
[35] R. Blume, M. Hävecker, S. Zafeiratos, D. Teschner, E. Kleimenov, A. Knop-Gericke, R. Schlögl, A. Barinov, P. Dudin, M. Kiskinova, J. Catal. 239 (2006) 354.
[36] B. Yang, S. Shaikhutdinov, H.-J. Freund, Surf. Sci. 632 (2015) 9.
[37] P. Banerjee, R. Woo, S. Grayson, A. Majumder, R. Raman, Influence of zeolite coating on the corrosion resistance of AZ91D magnesium alloy, 72014. 6092.
[38] P.V. Krivenko, S.G. Guziy, Appl. Clay Sci. 73 (2013) 65.
[39] Y. Wang, Y. Wu, L. Cheng, L. Zhang, J. Am. Ceram. Soc. 93 (2010) 204.
[40] H.E. Eaton, T.H. Lawton, Barium-strontium aluminosilicate protective coating for silicon containg substrate which inhibits the formation of cracks and the formation of silicon gases when the article is exposed to a high temperature, aqueous environment, in, Google Patents, 2002.
[41] J. Djordjevic, V. Dondur, R. Dimitrijevic, A. Kremenovic, Phys. Chem. Chem. Phys. 3 (2001) 1560.
[42] J.A. Boscoboinik, X. Yu, B. Yang, S. Shaikhutdinov, H.-J. Freund, Microporous Mesoporous Mater. 165 (2013) 158.